# Title: A *De Novo* Gain-of-Function Variant of *DNM1L* Causes Developmental Encephalopathy

Shangsheng Dong[1,*], Yanjuan Chen[1,*], Mengfang Yan[2,3,4,*], Xiaoli Huang[1], Qiannan Deng[5], Jianxiang Liao[6], Ke Zhang[2,4,5,#]

[1] Children's Health Rehabilitation Center, Jiangmen Maternal and Child Health Hospital, Jiangmen, Guangdong 529000, China, P.R.

[2] Shenzhen Medical Academy of Research and Translation Ph.D. Program, Shenzhen, Guangdong, 518107, China, P.R.

[3] Ph.D. Program, Westlake University, Hangzhou, Zhejiang 310024, China, P.R.

[4] Institute of Neurological and Psychiatric Disorders, Shenzhen Bay Laboratory, Shenzhen, Guangdong 518132, China, P.R.

[5] Rare Disease Center, Shenzhen Medical Academy of Research and Translation and Shenzhen Bay Laboratory, Shenzhen, Guangdong 518107, China, P.R.

[6] Department of Neurology, Shenzhen Children’s Hospital, Shenzhen, Guangdong 518026, China, P.R.

**#Correspondence to:**

Ke Zhang, Institute of Neurological and Psychiatric Disorders, Shenzhen Bay Laboratory, Shenzhen, Guangdong, 518107, China, P.R. Email: ke.zhang@szbl.ac.cn.

**Highlights:**

A novel heterozygous *DNM1L* variant causes developmental encephalopathy.

This variant causes intron retention, leading to a mutant protein.

Mutant Drp1 forms aggregates, disrupts mitochondria, and induces cytotoxicity via a gain-of-function mechanism.

Mutant Drp1 can confer toxicity to the wild-type protein.

**Abstract:**

**Background:** Variants in the *dynamin 1-like* (*DNM1L*) gene, which encodes dynamin-related protein 1 (Drp1), can cause encephalopathy due to defective mitochondrial and peroxisomal fission 1 (EMPF1) and optic atrophy 5 (OPA5), two neurodevelopmental disorders with distinct symptoms. Given the critical role of Drp1 in mitochondrial fission, it is believed that disrupted mitochondrial fission is key to EMPF1 and OPA5 pathogenesis. However, it is unclear whether other cellular defects also contribute to pathogenesis.

**Results:** Here, we report a novel *DNM1L* variant (c.1994+3T>G) in an EMPF1 patient with delayed psychomotor development, microcephaly, and hypotonia but without epilepsy. This *de novo*, heterozygous, and intronic variant causes the retention of a *DNM1L* intron, leading to an aberrant Drp1 protein with a gain of toxicity. Mechanistic studies suggested that the mutant Drp1 forms aggregates and disrupts mitochondrial morphology in cultured cells. Compared to expressing the mutant protein alone, co-expressing both wild-type and mutant Drp1 causes defects at a similar level, suggesting that the mutant Drp1 can confer toxicity to wild-type proteins.

**Conclusions:** Combined, our findings broadened the spectrum of pathogenic *DNM1L* variants and suggested protein aggregation as a potentially novel pathogenic contributor.

**Key Words:** neurodevelopmental disorders, *DNM1L*, mitochondria, protein

aggregate,

## BACKGROUND

Variants in *dynamin 1-like* (*DNM1L*) can cause two distinct neurodevelopmental disorders: encephalopathy due to defective mitochondrial and peroxisomal fission 1 (EMPF1, OMIM #614388) and optic atrophy 5 (OPA5, OMIM#610708). EMPF1 is characterized by delayed psychomotor development and hypotonia, sometimes associated with seizures, cerebral atrophy, lactic acidosis, etc. OPA5 is a nonsyndromic form of optic atrophy characterized by slowly progressive visual loss, sometimes also associated with central scotoma and color vision defects.

Depending on the function of the *DNM1L* variants, EMPF1 can be either autosomal dominant or recessive. However, OPA5 is autosomal dominant. Both loss-of-function (LoF) and gain-of-function (GoF) variants of *DNM1L* have been identified, with the latter sometimes showing a dominant negative effect, suggesting that loss of *DNM1L* function causes pathogenesis.

*DNM1L* encodes dynamin-related protein 1 (Drp1), a GTP-hydrolyzing dynamin protein conserved from yeast to human. It plays an essential role in mitochondrial fission (Kalia et al., 2018), a critical process for mitochondrial structure and function. Drp1 has an N-terminal GTPase domain, a middle domain, a variable domain (VD), and a C-terminal GTPase effector domain

(GED). More than 90% of the pathogenic variations are found in the GTPase and middle domains; the others are found in the VD and GED domains (Zhang et al., 2024). Most Drp1 variations are missense and dominant, with putative dominant-negative effects (Assia Batzir et al., 2019; Chao et al., 2016; Fahrner et al., 2016; Gerber et al., 2017; Vanstone et al., 2016; Waterham et al., 2007; Zhang et al., 2024). Only one missense (S36G) and two deletions in the GTPase domain are recessively inherited, suggesting LoF effects (Nasca et al., 2016; Yoon et al., 2016).

Here, we characterized a novel pathogenic *DNM1L* variant (NM_01206205: c.1994+3T>G), which was found heterozygous in a child patient with delayed psychomotor development, microcephaly, hypotonia, etc., but not in his parents. cDNA analyses suggested retention of intron #17 in the mRNA, leading to a frame-shift and premature stop. When overexpressed in cultured cells, the predicted mutant Drp1 exerts strong cytotoxicity, forms intracellular aggregates, and disrupts mitochondrial morphology. Furthermore, co-expressing the wild-type and predicted mutant Drp1 causes cytotoxicity similar to the mutant Drp1 alone, suggesting that the mutant Drp1 can convert wild-type proteins to be toxic. Combined, these data suggested a GoF mechanism. These findings expanded the genotypic spectrum of DNM1L-related disorders and suggested protein aggregation as a potential pathogenic contributor.

## METHODS

### mRNA extraction and RT-PCR

Total mRNA was extracted from peripheral blood samples using the TRIzol Reagent (Takara) and reverse-transcribed using iScript cDNA Synthesis Kit (Bio-Rad) following the manufacturer's instructions. PCR amplification was performed using the following primers: exon17-F: GGAGGTGGTGGGGTTGGAGAT and exon19-R: CCTCACAATCTCGCTGTTCCCGA.

### Molecular cloning

The wild-type and mutant *DNM1L* cDNA sequences were PCR-amplified from a cDNA clone using the following primers:

DNM1L-WT-F: GATTCTAGAGCTAGCGAATTCATGGAGGCGCTAATTCCTGTC

DNM1L-WT-R: ATCCTTCGCGGCCGCGGATCCTCACCAAAGATGAGTCTCCCGG

DNM1L-mutant-R:

TGCAACAGGAACTGGCTAAACCAAATTGTCATGGCTTAcCACATCTAGCAGGTT,

and the cDNA fragments were then cloned into the pCDH-CMV-MCS-EF1-copGFP-T2A-Puro vector using homologous recombination.

### Cell culture

U-2 OS cells were cultured in DMEM media (Gibco) supplemented with 10% fetal bovine serum (Sigma) and 1% penicillin-streptomycin (Gibco) at 37 °C.

Transfections were performed using Lipofectamine 3000 (Thermo Fisher Scientific), as indicated by the manufacturer's instructions. Twenty-four hours after transfection, cells were fixed for immunofluorescent staining or harvested and lysed for Western blots.

**Immunofluorescent staining**

Cells were fixed with 4% paraformaldehyde for 20 minutes, followed by permeabilization in PBX (PBS containing 0.1% Triton X-100) for 10 minutes. Subsequently, cells were incubated with primary antibodies against Drp1 (Proteintech, 26187-1-AP) and Tomm20 (Santa Cruz, sc-17764), each diluted 1:100 in the PBST wash buffer (PBS with 0.05% Tween-20) supplemented with 3% donkey serum, and left overnight at 4 °C. After incubation, cells were washed in PBST at room temperature. Donkey secondary antibodies conjugated with Alexa-Fluor 568 or 647 (ThermoFisher) were used at 1:1,000 in PBST supplemented with 3% donkey serum for 3 hours at room temperature. The cells were then washed and stained with DAPI. Finally, samples were mounted in ProLong Antifade Gold containing DAPI (Invitrogen) and imaged using a PLAPON 60x/1.42 oil immersion objective on an Olympus FV3000 confocal microscope. Images were analyzed using Fiji/ImageJ (NIH).

**Protein extraction and immunoblot**

For total protein extraction, cells were harvested and lysed in the Laemmli

buffer, and the lysates were heated at 98 °C for 10 minutes. For Drp1 aggregation assays, cells were lysed in the radioimmunoprecipitation assay (RIPA) buffer, and the supernatant was collected as the RIPA-soluble fraction. The remaining pellet was washed once with the RIPA buffer and then redissolved in 2% SDS or the urea buffer (50 μM Tris, pH 7.4, 8 M urea, 2% SDS) to obtain the RIPA-insoluble fraction. Subsequently, protein samples were separated on 4%–15% SDS Mini-PROTEAN TGX Precast Gels (Bio-Rad) and transferred to nitrocellulose membranes. Primary antibodies used were Drp1 (Proteintech, 26187-1-AP) and β-Actin (Millipore, MAB1501), diluted 1:1,000 and 1:5,000, respectively, in TBST (TBS with 0.05% Tween 20) containing 5% milk. HRP-conjugated donkey secondary antibodies (Jackson ImmunoResearch) were diluted 1:2,000 in TBST with 5% milk.

**MTT assay**

The MTT assay was performed according to the manufacturer's protocol (Invitrogen).

**Statistical analysis**

Statistical analyses were performed using the GraphPad Prism 9.5.1 software. Tests used and levels of significance for each experiment are explained in the figure legends.

**RESULTS**

## Clinical profiles of the proband

We report a three-year-old boy with no family neurological history presenting with psychomotor developmental delay, microcephaly, and autism spectrum disorders. He was the second child in the family, with a full-term vaginal delivery. He presented with delayed development in gross motor skills, language, cognition, and communication from birth. He could walk independently at around two years old, yet with an unsteady gait and frequent falls. At age three, he exhibited a positive Gowers' sign, no calf muscle hypertrophy, soft limb muscles with reduced muscle strength (level V-), and slight hypotonia, with overall growth parameters below age norms (height < -3 SD; weight between -2 and -3 SD). At the same age, he started expressing a few words, such as the names of family members, but his overall verbal expression is limited. In addition, he was emotionally unstable and afraid of strangers and exhibited significant crying and refusal to make eye contact during examinations. He could follow simple action instructions but exhibited poor cognition.

His head circumference at birth was normal (35 cm) but increased slowly over the past three years. At three years old, he exhibited microcephaly (head circumference: 44 cm) with a normal head shape and electroencephalogram. Magnetic resonance imaging showed no obvious structural abnormalities, but myelination was slightly delayed (Figure 1).

Exome sequencing identified a *de novo* heterozygous variant in the 18$^{th}$ intron of *DNM1L* (NM_012062.5: c.1994+3T>G) (Figure 2A), suggesting a dominant inheritance. According to gnomAD, this variant has a frequency of $3.40\times10^{-3}$ and is designated as a variant of uncertain significance. No other likely pathogenic variations were noted.

**The *DNM1L* c.1994+3T>G Variant Disrupts RNA Splicing**

Given that the variation of the patient is within an intron, we hypothesize that it disrupts splicing. To test this hypothesis, we extracted whole mRNA from patient blood cells, generated the whole cDNA, and PCR-amplified a *DNM1L* cDNA fragment containing exons 17, 18, and 19. As shown in Figure 2B, agarose gel electrophoresis analyses showed a larger-than-normal fragment present in the patient but not in any parents, suggesting intron retention, which was confirmed by Sanger sequencing (Figure 2C). Surprisingly, intron 17, but not 18, was retained in the variant cDNA despite the variation residing in intron 18.

*DNM1L* intron 17 encodes a seven-amino-acid peptide VSHDNLV, followed by a TAG stop codon. Thus, this *DNM1L* variant encodes a mutant protein truncated in the middle of the GED domain, with an additional VSHDNLV sequence at its C-terminus (Figure 2D), which we consider a GED domain variant.

**The Mutant Drp1 Causes Cytotoxicity and Mitochondrial Defects**

Next, we examined the function of our variant. We engineered cDNA constructs expressing either the wild-type or our mutant Drp1, transiently expressed these proteins in U-2 osteosarcoma cells, and performed the MTT cell viability assay. As expected, the mutant Drp1 is ~10 kD smaller than the wild type (Figure 3A). When the two proteins were expressed at comparable abundance (Figure 3A), the mutant Drp1 reduced cell viability by ~60%, whereas the wild-type Drp1 did not affect cell viability (Figure 3B), suggesting that the mutant is GoF. Interestingly, co-expressing the wild-type and mutant Drp1 reduced cell viability by a similar level compared to the mutant Drp1 alone (Figure 3B), suggesting that wild-type Drp1 does not suppress mutant Drp1 toxicity. In summary, our mutant Drp1 causes cytotoxicity that is not suppressed by overexpressing wild-type Drp1.

Drp1 localizes to the mitochondrial outer membrane, where it promotes mitochondrial fission (Otsuga et al., 1998). Defects in Drp1 cause disrupted mitochondrial morphology, as indicated by elongated, fused mitochondria. Thus, we examined mitochondrial morphology in cells expressing the wild-type and/or our mutant Drp1 using immunofluorescent staining on Tom20, a mitochondrial outer membrane marker. As shown in Figure 4A, transiently overexpressing the wild-type Drp1 causes fragmented mitochondria,

consistent with its role in promoting mitochondrial fission. Furthermore, overexpressing the mutant Drp1 causes long, fused mitochondria (Figure 4A and B), a phenotype mimicking Drp1 LoF (Taguchi et al., 2007), thereby suggesting a dominant-negative effect. Also, co-expressing wild-type and mutant Drp1 causes similar effects compared to mutant Drp1 alone, consistent with our cell viability results. Combined, our findings suggest that the mutant Drp1 disrupts mitochondrial morphology and causes cytotoxicity via dominant-negative effects.

**The Mutant Drp1 Forms Aggregates**

To better understand how the mutant Drp1 causes cytotoxicity, we co-stained cells overexpressing Drp1 with Tom20 and Drp1 antibodies. As shown in Figure 4A, the wild-type Drp1 forms a diffused pattern in cells, partially overlapping with Tom20 staining. Interestingly, the mutant Drp1 forms large puncta in the cytoplasm, sometimes in the vicinity of mitochondria, suggesting protein aggregation (Figure 4A). Agreeing with this idea, the wild-type Drp1 is RIPA-buffer-soluble, whereas most mutant Drp1 proteins are RIPA-insoluble and SDS- or urea-soluble (Figure 5A and B). Furthermore, co-expressing wild-type and mutant Drp1 causes some wild-type proteins to become RIPA-insoluble but SDS-soluble (Figure 5A), suggesting that the mutant Drp1 causes wild-type proteins to aggregate, consistent with a dominant-negative effect.

## DISCUSSION

Impaired mitochondrial fission is a critical pathogenic event in EMPF1. Here, we identify a de novo intronic *DNM1L* variant (c.1994+3T>G) affecting mitochondrial morphology in an EMPF1 patient. Mechanistic studies suggested that this variant causes cytotoxicity via a novel, GoF mechanism, as it causes intron retention, producing an aggregable, cytotoxic Drp1 that disrupts mitochondrial morphology. Remaining questions include whether Drp1 aggregates contribute to pathogenesis and can be a potential therapeutic target.

Previous studies identified most *DNM1L* pathogenic variations within the GTPase and middle domains, with a few variations within the GED domain (Zhang et al., 2024). Variations in the middle domain are frequently associated with EMPF1 and present with severe defects in the central nervous system (CNS), such as early-onset epileptic encephalopathy (Chao et al., 2016; Fahrner et al., 2016; Sheffer et al., 2016; Vanstone et al., 2016; Waterham et al., 2007). However, variations in the GED domain, including the one reported here, are associated with EMPF1 with mild symptoms, e.g., delayed psychomotor development with no obvious brain MRI defects (Assia Batzir et al., 2019; Nolden et al., 2022; Zhang et al., 2024). In addition, variations in the GTPase domain can be associated with either EMPF1 with

severe CNS defects or OPA5, an eye disease (Barbet et al., 2005; Gerber et al., 2017; Nasca et al., 2016; Yoon et al., 2016). Future studies can focus on the structure and function of Drp1 protein domains to better understand the genotype-phenotype correlation.

Most *DNM1L* variants associated with EMPF1 exhibit dominant-negative effects, as indicated by elongated, tubular mitochondria due to impaired mitochondrial fission (Berti et al., 2024; Hogarth et al., 2018; Javed et al., 2024; Nolden et al., 2022; Tarailo-Graovac et al., 2019). Here, we identify a novel, intronic variant in *DNM1L* that produces an aberrant, cytotoxic Drp1. In addition to disrupting mitochondrial fission, this aberrant protein forms aggregates and co-aggregates with the wild-type protein, rendering the latter cytotoxic. Thus, these findings suggested a toxic GoF mechanism.

A previous study showed that a K679A variation in the GED domain enhances Drp1 oligomer stability, likely by impairing disassembly rather than promoting assembly (Zhu et al., 2004). Consistent with this finding, we identified another variation within the GED domain, which causes Drp1 aggregation. Furthermore, Nolden et al. (2022) reported an EMPF1 patient with a p.Arg710Gly variation in the same domain, which causes aberrant Drp1 oligomerization (Nolden et al., 2022). Hence, these findings collectively suggested the importance of the GED domain in Drp1 assembly

and disassembly.

Protein aggregation is a pathological hallmark in many neurological diseases. For example, Aβ and Tau aggregates are pathological hallmarks of Alzheimer's disease, as well as α-synuclein in Parkinson's disease and TDP-43 in amyotrophic lateral sclerosis and frontotemporal dementia (Hardy, 2006; Neumann et al., 2006; Ross and Poirier, 2004). These aggregates sequester interacting proteins, thereby disrupting many cellular processes and organelles. For example, Aβ and Tau cause endoplasmic reticulum (ER) stress, activate an unfolded protein response (UPR), and disrupt protein homeostasis in cells (Abisambra et al., 2013; Fonseca et al., 2014; Soejima et al., 2013). TDP-43 sequesters nucleocytoplasmic transport factors, disrupting nucleocytoplasmic transport (Chou et al., 2018). Furthermore, misfolded TDP-43 is present in mitochondria and impairs their function, producing excessive reactive oxygen species and eventually causing apoptosis (Ruan et al., 2017). Drp1 aggregates may cause similar defects.

Protein aggregates could be disaggregated by molecular chaperones, such as Hsp70 and 90, or cleared by the proteasome or autophagy (Klaips et al., 2018; Mogk et al., 2018). Thus, activating chaperones, the proteasome, or autophagy mitigates misfolded protein stress, thereby ameliorating

neurological defects in many disease models (Xilouri et al., 2013) (Mogk et al., 2018). It is promising to test whether similar approaches suppress neurological defects in EMPF1 associated with protein aggregation.

## CONCLUSION

Our findings identified a novel pathogenic *DNM1L* variant causing neurodevelopmental defects and suggested protein aggregation as a potential pathogenic contributor.

## LIST OF ABBREVIATIONS

*DNM1L: dynamin 1-like*

Drp1: dynamin-related protein

EMPF1: encephalopathy due to defective mitochondrial and peroxisomal fission 1

OPA5: optic atrophy 5

LoF: loss of function

GoF: gain of function

VD: variable domain

GED: GTPase effector domain

CNS: central nervous system

## DECLARATIONS

### Ethics approval and consent to participate

The ethics of this study were approved by the ethics committee at Jiangmen Maternal and Child Health Hospital with the reference number of 2025079.

## Consent for publication

The patient's parents have signed the consent for publication.

**Availability of data and materials:** All data generated or analyzed during this study are included in this published article.

**Competing interests:** The authors declare no competing interests.

**Funding:** K.Z. is supported by the Guangdong Basic and Applied Basic Research Foundation (2023B1515020109) and the Major Program of Shenzhen Bay Laboratory (S241101003).

**Authors' contributions:** Conception: Y.C., J.L., K.Z.; Design: Y.C., K.Z.; Clinical data acquisition and analysis: S.D., Y.C., X.H., K.Z.; Laboratory data acquisition and analysis: M.Y., Q.D., K.Z.; Interpretation: Y.C., K.Z.; Writing: M.Y., K.Z. with the help of X.H.

**Acknowledgements:** We are grateful to the patient and his family. We thank Peng Han, Jing Yang, and Fanjia Hou for technical support. We thank the Biological Sample Repository and the Biom-Imaging Core at Shenzhen Bay Laboratory.

## FIGURE CAPTIONS

Figure 1. Brain magnetic resonance images of the patient at age three.

Figure 2. The *DNM1L* variant causes intron 17 retention.

Figure 3. The mutant Drp1 causes cytotoxicity.

Figure 4. The mutant Drp1 causes mitochondrial defects.

Figure 5. The mutant Drp1 forms aggregates.

## FIGURE LEGENDS

**Figure 1. Brain magnetic resonance images of the patient at age three.** (A) T1-weighted axial image. (B) T2-weighted axial image. (C) T2 fluid-attenuated inversion recovery (FLAIR)-weighted axial image. Red arrowheads indicate delayed myelination.

**Figure 2. The *DNM1L* variant causes intron 17 retention.** (A) The *DNM1L* gene structure. The arrowhead indicates the patient variant. (B) Agarose gel electrophoresis of PCR-amplified cDNA from the patient and his parents, with the normal and abnormal bands indicated respectively by the black and red arrowheads. (C) Sanger sequencing of an aberrant, PCR-amplified cDNA fragment from the patient. The blue part is intron 17. (D) Mutant Drp1 protein. The arrowhead indicates a stop codon.

**Figure 3. The mutant Drp1 causes cytotoxicity.** (A) Western blots of U-2 OS cells that are non-transfected or transfected with wild-type (WT), mutant (Mut), or both WT and Mut Drp1 for 24 hours. (B) Cell viability was assessed by MTT assay. One-way ANOVA (B). Means ± SEM. ns, not significant. $^{**}p < 0.01$, $^{***}p < 0.001$, and $^{****}p < 0.0001$.

**Figure 4. The mutant Drp1 causes mitochondrial defects.** (A) U-2 OS cells transiently expressing wild-type (WT, left), mutant (Mut, middle), or both WT and Mut (right) Drp1 were co-immunofluorescently stained with anti-Tom20 (green) and anti-Drp1 antibodies (red) and DAPI (blue). Inlets: GFP (white) indicates transfected cells. (B) Quantification of the mitochondrial morphology. *N* numbers on the graph. χ-square tests. ns, not significant. $^{****}p < 0.0001$.

**Figure 5. The mutant Drp1 forms aggregates.** (A) Western blots of RIPA-soluble and SDS-soluble fractions of cell lysates. Quantified below. (B) Western blots of RIPA-soluble and urea-soluble fractions of cell lysates. Quantified on the right. One-way ANOVA. Means ± SEM. $^{**}p < 0.01$.

## REFERNCES

Abisambra, J.F., Jinwal, U.K., Blair, L.J., O'Leary, J.C., 3rd, Li, Q., Brady, S., Wang, L.,

Guidi, C.E., Zhang, B., Nordhues, B.A.*, et al.* (2013). Tau accumulation activates the unfolded protein response by impairing endoplasmic reticulum-associated degradation. J Neurosci *33*, 9498-9507.

Assia Batzir, N., Bhagwat, P.K., Eble, T.N., Liu, P., Eng, C.M., Elsea, S.H., Robak, L.A., Scaglia, F., Goldman, A.M., Dhar, S.U.*, et al.* (2019). De novo missense variant in the GTPase effector domain (GED) of DNM1L leads to static encephalopathy and seizures. Cold Spring Harb Mol Case Stud *5*.

Barbet, F., Hakiki, S., Orssaud, C., Gerber, S., Perrault, I., Hanein, S., Ducroq, D., Dufier, J.L., Munnich, A., Kaplan, J.*, et al.* (2005). A third locus for dominant optic atrophy on chromosome 22q. J Med Genet *42*, e1.

Berti, B., Verrigni, D., Nasca, A., Di Nottia, M., Leone, D., Torraco, A., Rizza, T., Bellacchio, E., Legati, A., Palermo, C.*, et al.* (2024). De Novo DNM1L Mutation in a Patient with Encephalopathy, Cardiomyopathy and Fatal Non-Epileptic Paroxysmal Refractory Vomiting. Int J Mol Sci *25*.

Chao, Y.H., Robak, L.A., Xia, F., Koenig, M.K., Adesina, A., Bacino, C.A., Scaglia, F., Bellen, H.J., and Wangler, M.F. (2016). Missense variants in the middle domain of DNM1L in cases of infantile encephalopathy alter peroxisomes and mitochondria when assayed in Drosophila. Hum Mol Genet *25*, 1846-1856.

Chou, C.C., Zhang, Y., Umoh, M.E., Vaughan, S.W., Lorenzini, I., Liu, F., Sayegh, M., Donlin-Asp, P.G., Chen, Y.H., Duong, D.M.*, et al.* (2018). TDP-43 pathology disrupts nuclear pore complexes and nucleocytoplasmic transport in ALS/FTD. Nat Neurosci *21*, 228-239.

Fahrner, J.A., Liu, R., Perry, M.S., Klein, J., and Chan, D.C. (2016). A novel de novo dominant negative mutation in DNM1L impairs mitochondrial fission and presents as childhood epileptic encephalopathy. Am J Med Genet A *170*, 2002-2011.

Fonseca, A.C., Oliveira, C.R., Pereira, C.F., and Cardoso, S.M. (2014). Loss of proteostasis induced by amyloid beta peptide in brain endothelial cells. Biochim Biophys Acta *1843*, 1150-1161.

Gerber, S., Charif, M., Chevrollier, A., Chaumette, T., Angebault, C., Kane, M.S., Paris, A., Alban, J., Quiles, M., Delettre, C.*, et al.* (2017). Mutations in DNM1L, as in OPA1, result in dominant optic atrophy despite opposite effects on mitochondrial fusion and fission. Brain *140*, 2586-2596.

Hardy, J. (2006). A hundred years of Alzheimer's disease research. Neuron *52*, 3-13.

Hogarth, K.A., Costford, S.R., Yoon, G., Sondheimer, N., and Maynes, J.T. (2018). DNM1L Variant Alters Baseline Mitochondrial Function and Response to Stress in a Patient with Severe Neurological Dysfunction. Biochem Genet *56*, 56-77.

Javed, Z., Shin, D.H., Pan, W., White, S.R., Elhaw, A.T., Kim, Y.S., Kamlapurkar, S., Cheng, Y.Y., Benson, J.C., Abdelnaby, A.E.*, et al.* (2024). Drp1 splice variants regulate ovarian cancer mitochondrial dynamics and tumor progression. EMBO Rep *25*, 4281-4310.

Kalia, R., Wang, R.Y., Yusuf, A., Thomas, P.V., Agard, D.A., Shaw, J.M., and Frost, A. (2018). Structural basis of mitochondrial receptor binding and constriction by DRP1. Nature *558*, 401-405.

Klaips, C.L., Jayaraj, G.G., and Hartl, F.U. (2018). Pathways of cellular proteostasis in

aging and disease. J Cell Biol *217*, 51-63.

Mogk, A., Bukau, B., and Kampinga, H.H. (2018). Cellular Handling of Protein Aggregates by Disaggregation Machines. Mol Cell *69*, 214-226.

Nasca, A., Legati, A., Baruffini, E., Nolli, C., Moroni, I., Ardissone, A., Goffrini, P., and Ghezzi, D. (2016). Biallelic Mutations in DNM1L are Associated with a Slowly Progressive Infantile Encephalopathy. Hum Mutat *37*, 898-903.

Neumann, M., Sampathu, D.M., Kwong, L.K., Truax, A.C., Micsenyi, M.C., Chou, T.T., Bruce, J., Schuck, T., Grossman, M., Clark, C.M.*, et al.* (2006). Ubiquitinated TDP-43 in frontotemporal lobar degeneration and amyotrophic lateral sclerosis. Science *314*, 130-133.

Nolden, K.A., Egner, J.M., Collier, J.J., Russell, O.M., Alston, C.L., Harwig, M.C., Widlansky, M.E., Sasorith, S., Barbosa, I.A., Douglas, A.G.*, et al.* (2022). Novel DNM1L variants impair mitochondrial dynamics through divergent mechanisms. Life Sci Alliance *5*.

Otsuga, D., Keegan, B.R., Brisch, E., Thatcher, J.W., Hermann, G.J., Bleazard, W., and Shaw, J.M. (1998). The dynamin-related GTPase, Dnm1p, controls mitochondrial morphology in yeast. J Cell Biol *143*, 333-349.

Richards, S., Aziz, N., Bale, S., Bick, D., Das, S., Gastier-Foster, J., Grody, W.W., Hegde, M., Lyon, E., Spector, E.*, et al.* (2015). Standards and guidelines for the interpretation of sequence variants: a joint consensus recommendation of the American College of Medical Genetics and Genomics and the Association for Molecular Pathology. Genet Med *17*, 405-424.

Ross, C.A., and Poirier, M.A. (2004). Protein aggregation and neurodegenerative disease. Nat Med *10 Suppl*, S10-17.

Ruan, L., Zhou, C., Jin, E., Kucharavy, A., Zhang, Y., Wen, Z., Florens, L., and Li, R. (2017). Cytosolic proteostasis through importing of misfolded proteins into mitochondria. Nature *543*, 443-446.

Sheffer, R., Douiev, L., Edvardson, S., Shaag, A., Tamimi, K., Soiferman, D., Meiner, V., and Saada, A. (2016). Postnatal microcephaly and pain insensitivity due to a de novo heterozygous DNM1L mutation causing impaired mitochondrial fission and function. Am J Med Genet A *170*, 1603-1607.

Soejima, N., Ohyagi, Y., Nakamura, N., Himeno, E., Iinuma, K.M., Sakae, N., Yamasaki, R., Tabira, T., Murakami, K., Irie, K.*, et al.* (2013). Intracellular accumulation of toxic turn amyloid-beta is associated with endoplasmic reticulum stress in Alzheimer's disease. Curr Alzheimer Res *10*, 11-20.

Taguchi, N., Ishihara, N., Jofuku, A., Oka, T., and Mihara, K. (2007). Mitotic phosphorylation of dynamin-related GTPase Drp1 participates in mitochondrial fission. J Biol Chem *282*, 11521-11529.

Tarailo-Graovac, M., Zahir, F.R., Zivkovic, I., Moksa, M., Selby, K., Sinha, S., Nislow, C., Stockler-Ipsiroglu, S.G., Sheffer, R., Saada-Reisch, A.*, et al.* (2019). De novo pathogenic DNM1L variant in a patient diagnosed with atypical hereditary sensory and autonomic neuropathy. Mol Genet Genomic Med *7*, e00961.

Vanstone, J.R., Smith, A.M., McBride, S., Naas, T., Holcik, M., Antoun, G., Harper, M.E., Michaud, J., Sell, E., Chakraborty, P.*, et al.* (2016). DNM1L-related

mitochondrial fission defect presenting as refractory epilepsy. Eur J Hum Genet *24*, 1084-1088.

Waterham, H.R., Koster, J., van Roermund, C.W., Mooyer, P.A., Wanders, R.J., and Leonard, J.V. (2007). A lethal defect of mitochondrial and peroxisomal fission. N Engl J Med *356*, 1736-1741.

Xilouri, M., Brekk, O.R., Landeck, N., Pitychoutis, P.M., Papasilekas, T., Papadopoulou-Daifoti, Z., Kirik, D., and Stefanis, L. (2013). Boosting chaperone-mediated autophagy in vivo mitigates alpha-synuclein-induced neurodegeneration. Brain *136*, 2130-2146.

Yoon, G., Malam, Z., Paton, T., Marshall, C.R., Hyatt, E., Ivakine, Z., Scherer, S.W., Lee, K.S., Hawkins, C., Cohn, R.D.*, et al.* (2016). Lethal Disorder of Mitochondrial Fission Caused by Mutations in DNM1L. J Pediatr *171*, 313-316 e311-312.

Zhang, Z., Bie, X., Chen, Z., Liu, J., Xie, Z., Li, X., Xiao, M., Zhang, Q., Zhang, Y., Yang, Y.*, et al.* (2024). A novel variant of DNM1L expanding the clinical phenotypic spectrum: a case report and literature review. BMC Pediatr *24*, 104.

Zhu, P.P., Patterson, A., Stadler, J., Seeburg, D.P., Sheng, M., and Blackstone, C. (2004). Intra- and intermolecular domain interactions of the C-terminal GTPase effector domain of the multimeric dynamin-like GTPase Drp1. J Biol Chem *279*, 35967-35974.

Figure 1

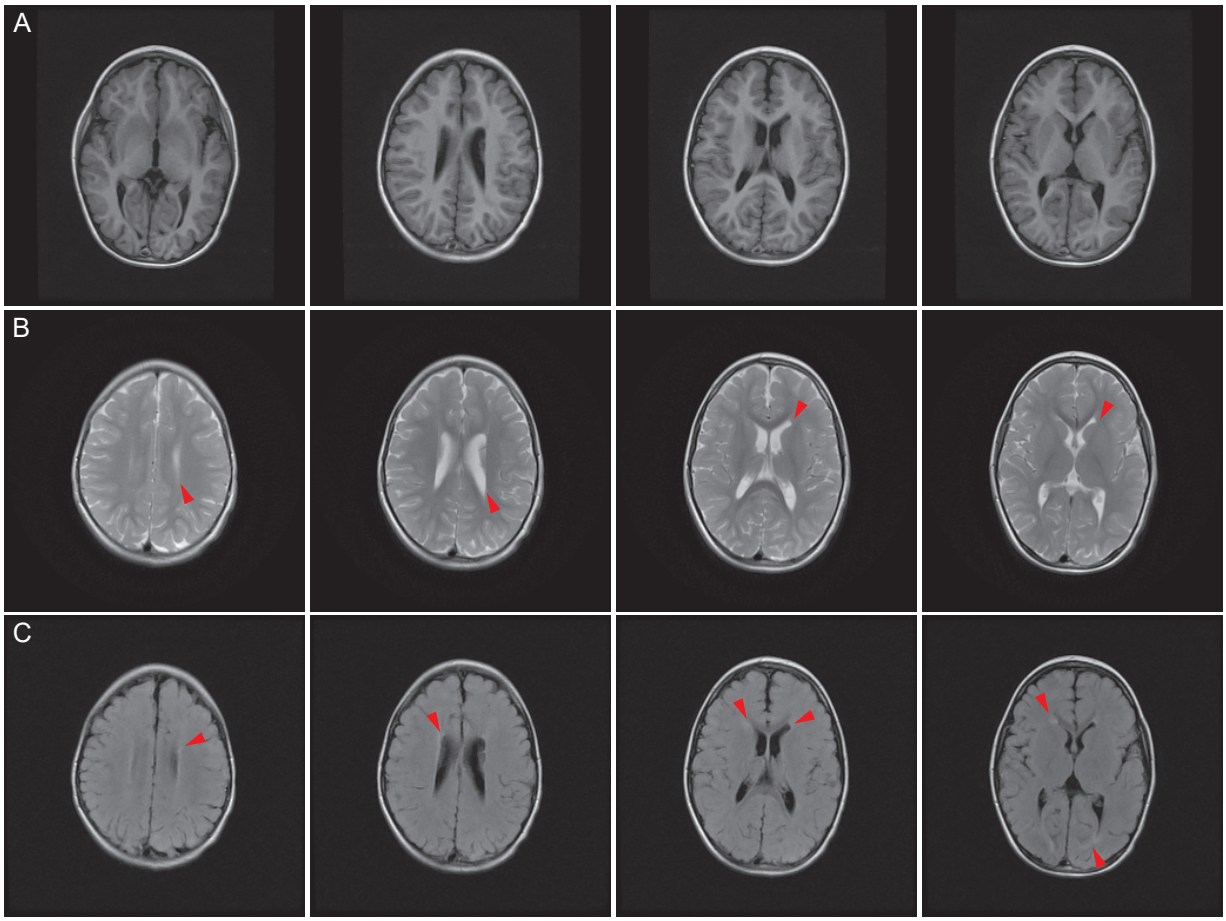

Figure 2

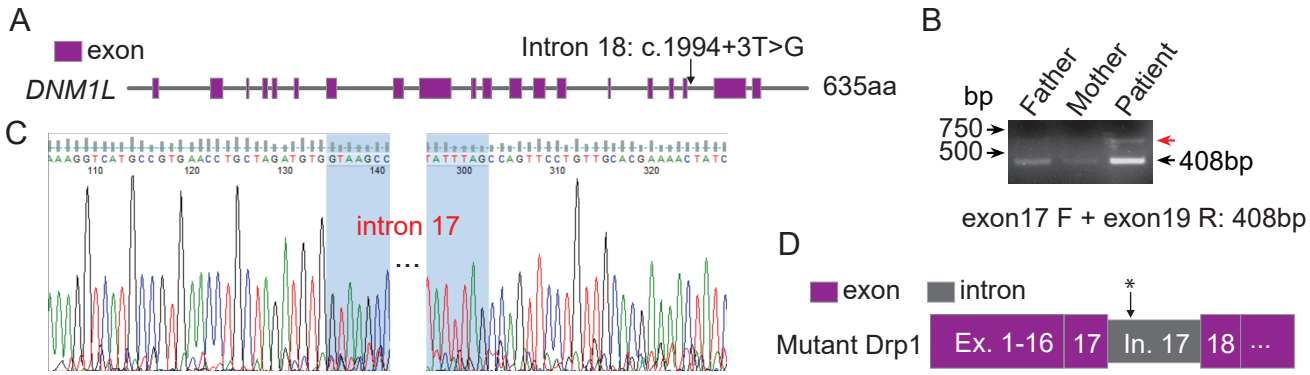
A
exon
DNM1L
Intron 18: c.1994+3T>G
635aa
B
bp
Father
Mother
Patient
750
500
408bp
exon17 F + exon19 R: 408bp
C
intron 17
D
exon
intron
Mutant Drp1
Ex. 1-16
17
In. 17
18
...

Figure 3

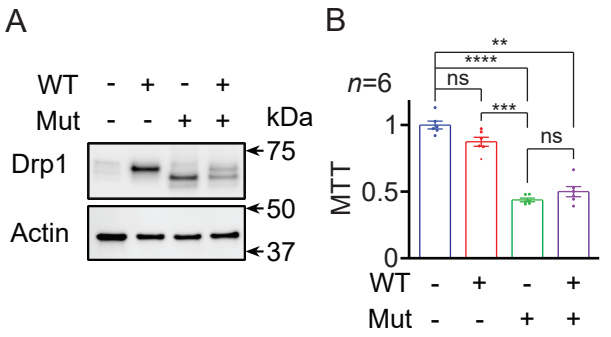

Figure 4

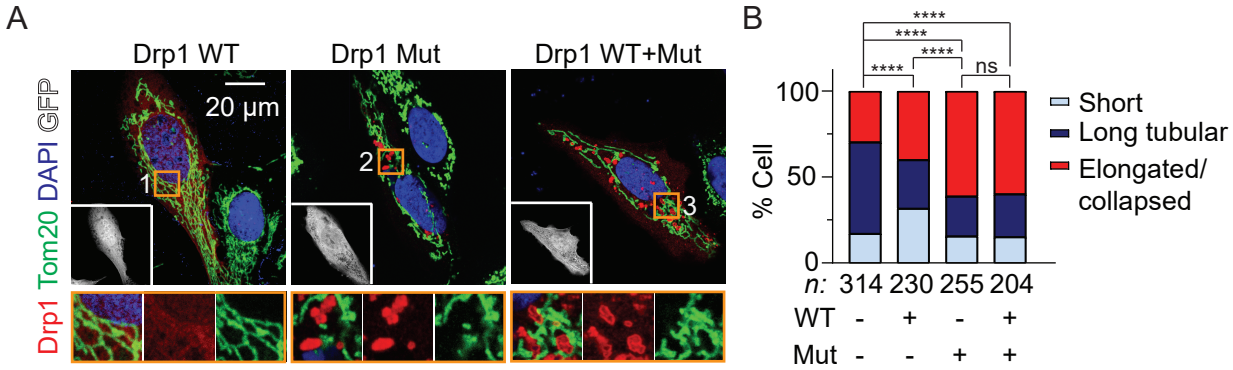
A
Drp1 WT
Drp1 Mut
Drp1 WT+Mut
20 µm
1
2
3
Drp1 Tom20 DAPI GFP
B
****
****
****
****
ns
100
50
0
% Cell
n: 314 230 255 204
WT - + - +
Mut - - + +
Short
Long tubular
Elongated/
collapsed

Figure 5

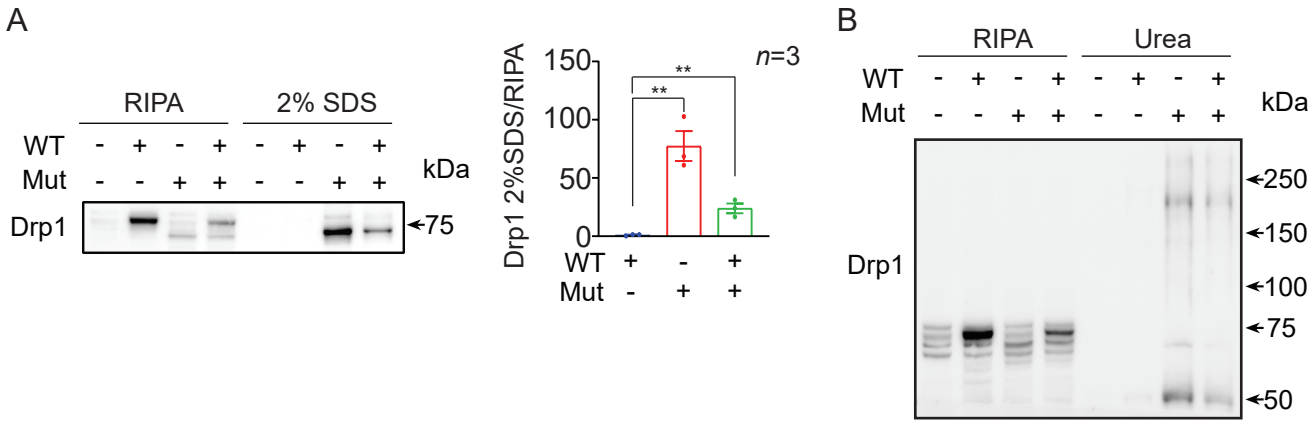
A
RIPA
2% SDS
WT - + - + - + - +
Mut - - + + - - + +
kDa
Drp1
75
Drp1 2%SDS/RIPA
150
100
50
0
**
**
n=3
WT + - +
Mut - + +
B
RIPA
Urea
WT - + - + - + - +
Mut - - + + - - + +
kDa
Drp1
250
150
100
75
50